PCCP

Cite this: *Phys. Chem. Chem. Phys.*, 2012, **14**, 8403–8409

www.rsc.org/pccp

PAPER

Heterogeneous reaction of acetic acid on MgO, α-Al_2O_3, and $CaCO_3$ and the effect on the hygroscopic behaviour of these particles†

Qingxin Ma, Yongchun Liu, Chang Liu and Hong He*

Received 18th February 2012, Accepted 2nd April 2012
DOI: 10.1039/c2cp40510e

Mixtures of organic compounds with mineral dust are ubiquitous in the atmosphere, whereas the formation pathways and hygroscopic behavior of these mixtures are not well understood. In this study, *in situ* DRIFTS, XRD, and a vapor sorption analyzer were used to investigate the heterogeneous reaction of acetic acid on α-Al_2O_3, MgO, and $CaCO_3$ particles under both dry and humid conditions while the effect of reactions on the hygroscopic behavior of these particles was also measured. In all cases, formation of acetate is significantly enhanced in the presence of surface water. However, the reaction extent varied with the mineral phase of these particles. For α-Al_2O_3, the reaction is limited to the surface with the formation of surface coordinated acetate under both dry and humid conditions. For MgO, the bulk of the particle is involved in the reaction and $Mg(CH_3COO)_2$ is formed under both dry and humid conditions, although it exhibits a saturation effect under dry conditions. In the case of $CaCO_3$, acetic acid uptake is limited to the surface under dry conditions while it leads to the decomposition of the bulk of $CaCO_3$ under humid conditions. While coordinated surface acetate species increased the water adsorption capacity slightly, the formation of bulk acetate promoted the water absorption capacity greatly. This study demonstrated that heterogeneous reaction between CH_3COOH and mineral dust is not only an important sink for CH_3COOH, but also has a significant effect on the hygroscopic behavior of mineral dust.

1. Introduction

Mineral aerosols, which originate from arid and semi-arid region, represent one of the largest mass fractions of global aerosols. The annual flux of mineral aerosol to the atmosphere is estimated to be about 1000–3000 Tg.[1,2] Mineral aerosols are considered as one of the largest uncertainties in predicting future climate change due to their complexity in climate effects.[3] They can affect climate directly by absorbing and scattering solar and terrestrial radiation, and indirectly by acting as cloud condensation nuclei (CCN).[4] The climate forcing effect of atmospheric particles greatly depends on their chemical composition. It is well known that mineral dust particles may transport over thousands of kilometers[5] and alter the chemical balance of the atmosphere by providing a reactive substrate or medium for pollution gases.[6–10] These reactions can not only change atmospheric trace gas distributions but also modify the composition and mixing state of particles, which then affect its thermodynamic and optical properties. Therefore, it is critical to thoroughly understand the effect of aging processes on the physicochemical properties of mineral particles for improving future climate prediction models.

On the other hand, the mixing state of an aerosol particle plays a critical role in its hygroscopicity, which then determines the size, water content, and optical properties of the particle. In field measurements, mixtures of mineral dust with nitrate, sulfate, and organic compounds have been frequently observed.[11–15] Laboratory studies have also confirmed that heterogeneous reaction on mineral dust particles can always enhance their hygroscopicity. For example, complete conversion of insoluble $CaCO_3$ to hygroscopic $Ca(NO_3)_2$ particles was observed when $CaCO_3$ particles were exposed to HNO_3 or NO_2 in humid conditions.[16–20] These processes result in a remarkable enhancement of water content and CCN activity of the aged particles.

Carboxylic acids are ubiquitous in the troposphere which has been frequently observed in precipitation, cloudwater and fogwater, the gaseous phase, and in particulate aerosols.[21] The sources of carboxylic acids comprise directly anthropogenic and biogenic emissions as well as secondary production from the photochemical oxidation of atmospheric hydrocarbons.[21–23] A major removal mechanism for atmospheric carboxylic acids is *via* wet deposition due to the large solubility and its role in the formation of CCNs.[24] Meanwhile, carboxylic acids in

Research Center for Eco-Environmental Sciences, Chinese Academy of Sciences, Beijing, 100085, China. E-mail: honghe@rcees.ac.cn; Fax: 86-10-6292-3563; Tel: 86-10-6284-9123
† Electronic supplementary information (ESI) available. See DOI: 10.1039/c2cp40510e

the atmosphere also showed a correlation with mineral aerosols in field studies.[25–29] The loss pathway involving dry deposition of carboxylic acids to mineral dust particles and surfaces has been partly simulated in laboratory studies.[30–35] Acetic acid (CH_3COOH, or HAc) is a major component of carboxylic acids and is always chosen as representative carboxylic acid in laboratory studies. The uptake coefficients of acetic acid on Fe_2O_3, Al_2O_3, and SiO_2 were measured with Knudsen cell/mass, and the calculated atmospheric lifetime due to heterogeneous uptake is close to that of photolysis.[30] By studying the heterogeneous uptake of the C_1 to C_4 organic acids on a swelling clay mineral under typical upper tropospheric temperatures and atmospherically relevant RH values, Hatch *et al.* estimated that approximately 40% of the gas phase acetic acid would be removed from the atmosphere.[32] Prince *et al.* found that the buffering capacity of the carbonate and the formation of soluble acetate product will provide a thermodynamic driving force for acetic acid partitioning to the particle phase in the presence of water.[34] Tong *et al.* calculated the atmospheric lifetimes of monocarboxylic acids contributed to heterogeneous reactions on α-Al_2O_3 at different relative humidities.[35] They found the calculated lifetimes of acetic acid are shorter than those for removal by reaction with OH.[35] Based on these previous results for mineral dust, we can conclude that heterogeneous chemistry involving mineral dust may be a significant sink for atmospheric acetic acid. However, little attention has been paid to the effect of these reactions on the hygroscopic behavior of particles.

α-Al_2O_3, MgO, and $CaCO_3$ are important reactive constituents of mineral dust and they were always chosen as substitute for mineral aerosol particles in laboratory studies. Therefore, in this study, α-Al_2O_3, MgO, and $CaCO_3$ were chosen as proxies for mineral dust to study the heterogeneous reactions of acetic acid on mineral dust as well as the effects on the hygroscopic behavior. Three aims of this study were as follows: firstly, to study the reaction mechanisms of acetic acid with various mineral particles; secondly, to elucidate the role of water on these reactions; thirdly, to determine the effect of these reactions on the hygroscopic behavior of particles.

2. Experimental

In situ diffuse reflectance infrared Fourier transform spectroscopy (DRIFTS) spectra were recorded on a NEXUS 670 (Thermo Nicolet Instrument Corporation) FT-IR, equipped with an *in situ* diffuse reflection chamber and a high-sensitivity mercury cadmium telluride (MCT) detector cooled by liquid N_2. The sample (about 11 mg) for the *in situ* DRIFTS studies was finely ground and placed into a ceramic crucible in the *in situ* chamber. The sample was first flushed by dry N_2 for 10 h at 300 K. After the reference spectrum was recorded, it was then exposed to reactant gases. The acetic acid gas was carried by dry N_2 through an acetic acid container and then mixed with dry or humid N_2. The concentration of acetic acid was calculated from the saturation pressure of acetic acid and the ratio of different N_2 flows. It was 1.4–1.5 $\times$ 10^{15} molecule/cm^3 (50–55 ppm) in all experiments. The relative humidity in flow reactor was controlled by adjusting the ratio of dry and humid N_2 flow. The infrared spectra were collected and analyzed using a data acquisition computer with OMNIC 6.0 software (Nicolet Corp.). All spectra reported here were recorded at a resolution of 4 cm^{-1} for 100 scans.

Hygroscopic behavior of particles was measured with a modified physisorption analyzer (Quartarnchrome, AUTOSORB-1S), which was described detailed in a previous study.[36] In a brief, vapor was used as adsorbate and the physisorption analyzer allows monitoring of the pressure change in the system during the adsorption process, which then could be converted to the mass of water uptake on particles. This instrument has been determined to be reliable for measuring the water content, deliquescence point, and monolayer forming point, as well as calculation of the growth factor of completely soluble particles.[36] The temperature of the sample station in this study was maintained at 278 K within $\pm$0.1 K by using a super thermostat and a cryofluid pump (DFY 5/80, Henan Yuhua laboratory instrument factory). Before adsorption experiment, all samples were pumped at 10^{-3} Torr for 2 h at room temperature. The water content at 90%RH was compared for particles since most growth factors of particles at 90%RH have been reported in the literature. For aged particles, the reaction processes were conducted in a flow reactor under the same experimental conditions as the DRIFTS study.

X-Ray diffraction (XRD) characterization was conducted with a computerized PANalytical X'Pert Pro X-ray Diffractometer (Netherlands) using Cu-Kα radiation and operating at 40 kV and 40 mA. The patterns were taken with the 2θ range from 10 to 80 at a scan speed of 4°/min. Peak positions and relative intensities were characterized by comparison with ICDD files. The aging process was the same as that of DRIFTS study.

Sources of Chemicals. The α-Al_2O_3 sample was prepared from boehmite (AlOOH, supplied by Shangdong Alumina Corporation) by calcining at 1473 K for 3 h. MgO (AR, Tianjin HANGU chemical factory) and $CaCO_3$ (AR, Beijing YILI chemical factory) were used as purchased. The specific areas were computed by applying the Brunauer–Emmett–Teller (BET) method from nitrogen adsorption–desorption isotherms which were obtained at 77 K. The surface areas are 11.5, 13.6 and 0.6 m^2 g^{-1} for fresh α-Al_2O_3, MgO and $CaCO_3$ particles, respectively. CH_3COOH (AR, >99%, Beijing chemical factory) was carried and diluted with N_2 (>99.999%, Beijing HUAYUAN gas Co., Ltd). Deionized water (18 mΩ) was degassed prior to use.

3. Results and discussion

3.1 DRIFTS study HAc adsorption on MgO and α-Al_2O_3 particles

Fig. 1A shows the spectra of HAc adsorption on MgO particles as a function of time at 300 K under dry condition (RH < 2%). Several peaks at 950, 1025, 1053, 1265, 1342, 1456, 1604, 1710, 2937, and 3014 cm^{-1} as well as negative peaks at 865, 3700, and 3740 cm^{-1} are observed. The intensities of these peaks increased with the exposure time. The peaks at 1710 cm^{-1} and 1265 cm^{-1} are assigned to the stretching mode of ν(C=O) and ν(C–OH) in residual acetic acid, respectively.[37] When the sample was flushed with dry

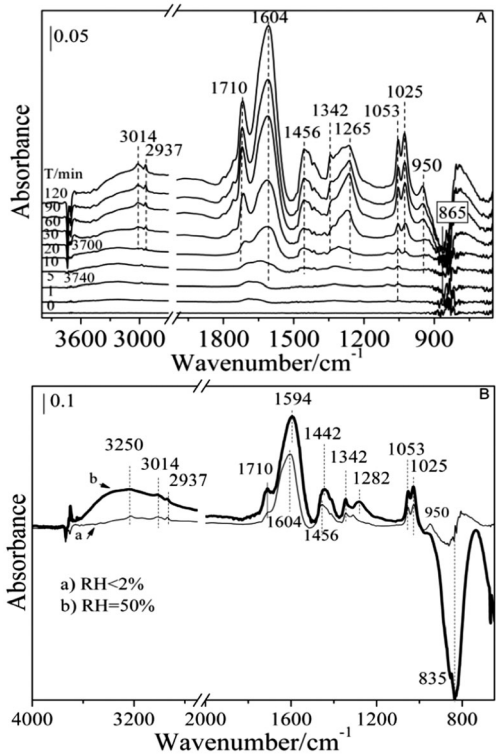

Fig. 1 (A) DRIFTS spectra of HAc adsorption on MgO under dry condition as a function of time; (B) The spectra of MgO particles reacted with HAc under (a) dry (RH < 2%) and (b) humid conditions (RH = 50%) for 2 h.

nitrogen after reaction, these two peaks decreased. The bands at 1604 and 1456 cm^{-1} are attributed to the asymmetric (ν_{as}(OCO)) and symmetric (ν_s(OCO)) stretching mode of the OCO group of acetate, respectively.[35] Other bands are assigned according to previous studies[35,37–39] and also summarized in Table 1. The negative peaks at 3700 and 3740 cm^{-1} are due to the consumption of hydroxyl on MgO surface.[40] Another negative peak at 865 cm^{-1} is supposed to the decomposition of MgO matrix indicating bulk MgO may be involved in this reaction.

At high RH (50%), the intensities of all the bands due to acetate species increased obviously when compared with those under dry condition, as seen in Fig. 1B. A broad band at a center of 3250 cm^{-1} is assigned to the stretching mode of adsorbed water on the particles. Another IR absorbance band

Table 1 Assignments of vibrational bands (cm^{-1}) of surface species formed when MgO were exposed to CH_3COOH

Bands/cm^{-1}	Mode	Ref.
3740	ν(O–H)	40
3700		
2937	$\nu(CH_3)$	35,39
3014		
1710	ν(C=O)	37
1265	ν(C–OH)	37
1608	ν_{as}(OCO	35
1456	ν_s(OCO)	
1342	$\delta_s(CH_3)$	37
1053	$\rho_{op}(CH_3)$	38,39
1025	$\rho_{ip}(CH_3)$	

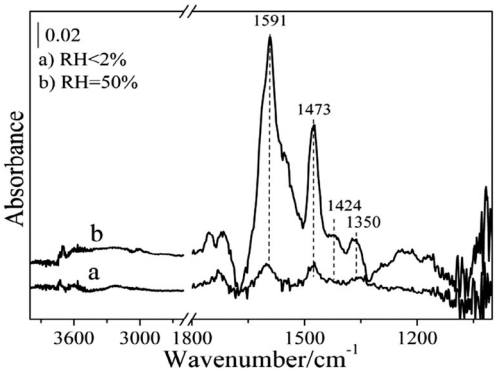

Fig. 2 The spectra of α-Al_2O_3 particles reacted with HAc under (a) dry (RH < 2%) and (b) humid conditions (RH = 50%) for 2 h.

at 835 cm^{-1} due to consumption of MgO shows an intense negative peak. It suggests that the presence of water promoted the decomposition of bulk MgO. It is interesting to note that the peaks due to CH_3 vibration show no peak shift, but the bands due to the asymmetric and symmetric stretching mode of OCO group exhibit a clear red shift from 1604 and 1456 cm^{-1} to 1594 and 1442 cm^{-1}, respectively. This red shift implies that the conversion of surface coordinated acetate to relative free acetate ions occurred in the presence of surface water.[38,39] Wang *et al.*[41] studied the dehumidifying process of $Mg(CH_3COO)_2$ droplet by Raman spectroscopy and observed a blue shift of peaks due to the OCO group. They attributed this shift to the conversion of free CH_3COO^- to a contact ions pair (CIPs) of Mg^{2+}–CH_3COO^-. Therefore, we inferred that the red shift may be due to the conversion of CIPs to free acetate ions in the presence of surface water.

Adsorption processes of HAc on α-Al_2O_3 under both dry and humid conditions (50% RH) were also monitored by DRIFTS. The α-Al_2O_3 samples were exposed to HAc for 2 h under dry or humid conditions (50% RH), and then purged with N_2 for 1 h. Fig. 2 only shows the final spectra of these two reacted particles for comparison. The peaks at 1591, 1473, 1424, and 1350 cm^{-1} are observed in both spectra. The former two peaks are attributed to the asymmetric and symmetric stretching mode of the OCO group of acetate,[30,35] while the later two peaks are assigned to C–H deformation.[35] These results indicate that acetate was formed on the α-Al_2O_3 surface. By FTIR, previous studies[30,35] found that uptake of HAc on α-Al_2O_3 exhibited irreversible adsorption and surface acetate was formed. The results in this study are consistent with these previous studies.[30,32,35] Increased intensities without a position shift of these peaks were observed when the adsorption process was conducted under humid conditions (RH = 50%). It suggests that the presence of surface water can promote the adsorbed HAc to form surface coordinated acetate species but cannot form bulk $Al(CH_3COO)_3$. In contrast to MgO particles, the reaction between HAc and α-Al_2O_3 was only limited to the surface but not involved the bulk. In a previous study of HAc adsorption on α-Al_2O_3 particles, Tong *et al.* also suggested that the bulk oxygen does not participate in the reaction and the reaction happens only on the surface.[35]

3.2 XRD characterization results

To further inspect the reaction extent, fresh and reacted particles were characterized by XRD. Fig. 3 shows the XRD

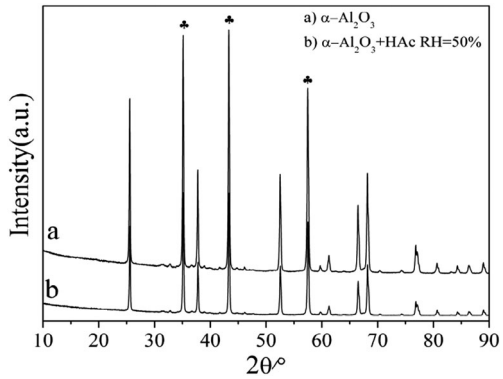

Fig. 3 XRD spectra of (a) α-Al_2O_3 and (b) α-Al_2O_3 reacted with HAc at 50% RH for 12 h.

spectra of α-Al_2O_3 particles before and after reaction with HAc under humid condition (50% RH) for 12 h. The three main peaks of fresh particles are 35.0°, 43.0°, and 57.0°, which is a feature of the alpha phase (ICDD 00-046-1212). When the particles were exposed to acetic acid at 50% RH, no position shift of these peaks is observed while only a small intensity decrease is observed. Although acetate species were observed in DRIFTS spectra (Fig. 2), no new peak in the XRD spectrum appeared. It indicates that no crystalline $Al(CH_3COO)_3$ was formed on α-Al_2O_3. Combined with DRIFTS results, we can conclude that the reaction of HAc on α-Al_2O_3 particles was limited to the surface and the bulk of the particle is not involved.

MgO particles showed different results from α-Al_2O_3 particles in XRD study, as seen in Fig. 4. The three main peaks of fresh MgO particles are 42.9°, 62.3°, and 78.6° (Fig. 4a), which is the characteristic of periclase phase (ICDD PDF 45 0496). The MgO particles, after reaction with HAc under dry condition, exhibited a similar spectrum to that of fresh MgO particles; nevertheless a broad band with a center at 24° was observed (Fig. 4b). This band was clearly seen in the spectrum of $Mg(CH_3COO)_2$ particles (Fig. 4d) which were produced by mixing MgO with acetic acid solution and then purging with dry N_2. This result indicates that crystallite of $Mg(CH_3COO)_2$ was formed on MgO surface in dry reaction. When the reaction was under humid conditions, the intensities of bands due to MgO crystalline decreased (Fig. 4c). It implies that the presence of surface water promoted the decomposition of MgO crystalline. By using transmission FT-IR spectroscopy, Al-Abadleh and Grassian[42] investigated the role of water in nitric acid uptake on MgO(100) at 296 K. They found that under dry conditions, nitric acid uptake is limited to the topmost surface layer and saturates at a single layer of magnesium nitrate. However, in the presence of water vapor at 25% relative humidity, subsurface layers can participate in the reaction while the extent of nitric acid uptake and the formation of magnesium nitrate is significantly enhanced on MgO(100) without evidence of saturation after 1 h of reaction. In the present study, a similar phenomenon for MgO reacted with HAc was observed. Both DRIFTS and XRD results demonstrated that decomposition of the bulk structure of MgO occurred during the reaction with HAc. However, the band due to crystalline $Mg(CH_3COO)_2$ does not increase. It may be due to the separation of Mg^{2+} and CH_3COO^- in the presence of residual surface water, and only amorphous $Mg(CH_3COO)_2$ internally mixed with MgO particles were formed (also see TGA result in ESI†).

We also characterized the acetic acid reacted $CaCO_3$ particles by XRD, as shown in Fig. 5. As shown in Fig. 5a, three main peaks of fresh $CaCO_3$ particles at 29.4, 39.4, and 48.4°, are the feature of calcite phase (ICDD 00-047-1743). No spectral change is observed for the $CaCO_3$ particles after reaction with HAc under dry conditions (Fig. 5b), indicating the reaction was limited to the surface. While the $CaCO_3$ particles were exposed to HAc at 50% RH for 12 h, the peaks related to calcite decreased markedly and some new peaks appeared (Fig. 5c). These new peaks do not match well up to the XRD features of the pure $Ca(CH_3COO)_2$ sample (Fig. 5d), which may be because the $Ca(CH_3COO)_2$ formed on $CaCO_3$ surface is not well-crystallized. There are plenty of previous studies on the uptake of acidic gases, such as HNO_3, NO_2, SO_2, CH_3COOH, and HCOOH, on $CaCO_3$ particles. Surface H_2CO_3 was found as a critical intermediate and it is stable under dry conditions.[43] The stable surface H_2CO_3 makes a further reaction between acidic gases and $CaCO_3$, being limited to the surface under dry condition. In contrast, when $CaCO_3$ particles were exposed to acidic gases in the presence of vapor, $CaCO_3$ particles can be decomposed.[31,34,44,45]

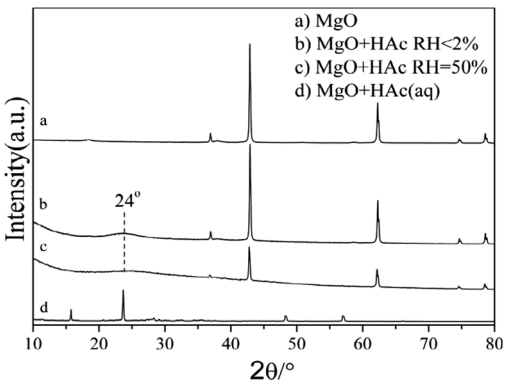

Fig. 4 XRD spectra of (a) fresh MgO and after reaction with HAc under (b) dry, (c) humid, and (d) aqueous condition. The reaction time is 12 h.

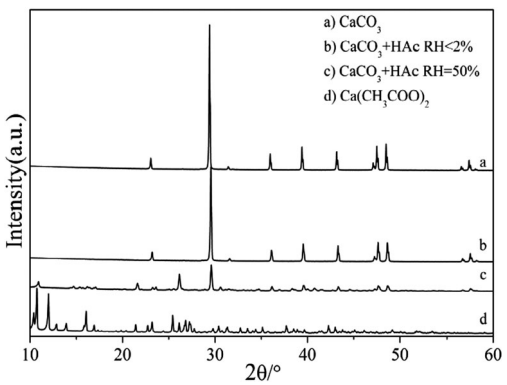

Fig. 5 XRD spectra of (a) fresh $CaCO_3$, reacted with HAc under (b) dry and (c) humid condition, and (d) $Ca(CH_3COO)_2$. The reaction time is 12 h.

Thus, in the present study, reaction between HAc and $CaCO_3$ particles showed no XRD spectra change under dry conditions. When surface water was present, decomposition of bulk $CaCO_3$ by HAc was facilitated, which was in good agreement with those previous results. As a result, conversion of calcite to internally mixed $Ca(CH_3COO)_2/CaCO_3$ happened.

3.3 Hygroscopic behaviour measurement

Although it is generally recognized that the aging process could change the hygroscopicity of aerosols, little attention has been paid to the hygroscopic behavior of internally mixed organic/mineral particles. In this study, we further made a comparison on water adsorption/absorption processes of fresh particles and acetic acid reacted particles by a modified vapor sorption analyzer.[36,46] Fig. 6 shows the water adsorption isotherms of fresh and acetic acid reacted α-Al_2O_3 particles. In order to obtain absolute values of surface coverage, the mass of water adsorbed was converted into coverage in terms of formal water monolayers by making a reasonable assumption about the size of the adsorbed water molecule (14.3 $Å^2$)[47] and knowing the surface area of the sample (11.5 $m^2\ g^{-1}$ from BET). The monolayer point of fresh α-Al_2O_3 particles is $\sim$20% RH, which is consistent with the results in other studies.[35,48] This point decreased to $\sim$14% RH for acetic acid reacted particles. A lower relative humidity, corresponding to one monolayer of water adsorbed, always refers to a higher hydrophilicity, thus these results suggest that reaction with HAc can enhance the hydrophilic properties of the particles. On the other hand, the water content at 90% RH also increased from 1.7% of fresh particles to 5.2% of reacted particles. However, no deliquescence was observed, indicating only a small amount of acetate exists on the surface. It is consistent with DRIFTS and XRD results that the reaction is limited to the surface.

Fig. 7 shows the water adsorption isotherms of fresh MgO and acetic acid reacted particles. The relative humidity corresponding to one monolayer of water adsorbed on MgO was measured to be $\sim$24%RH with the calculation method mentioned above. When the MgO particles were exposed to HAc under dry or humid conditions, the amount of adsorbed water was significantly enhanced. The relatively greater amount of adsorbed water makes calculation of the coverage layer unsuitable. Calculation of the growth factors is also impossible due to

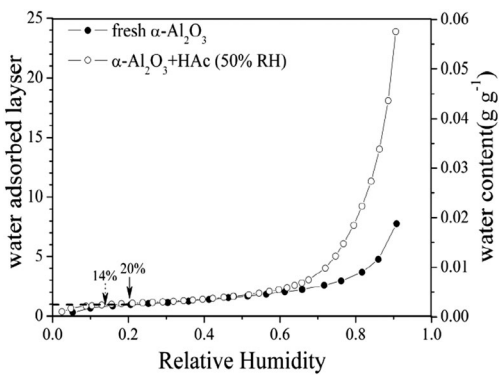

Fig. 6 Adsorption isotherms of water on fresh α-Al_2O_3 (solid) and acetic acid reacted particles (empty) at 278 K. The reaction time is 12 h.

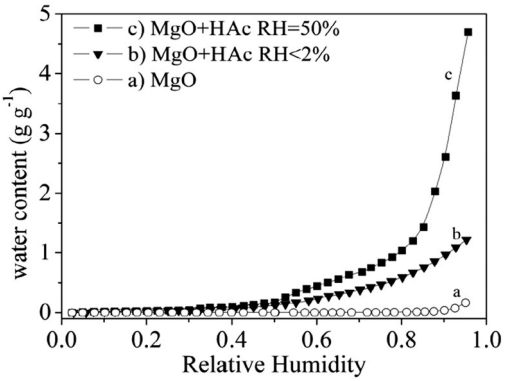

Fig. 7 Adsorption isotherms at 278 K of water on (a) fresh MgO and MgO reacted with HAc under (b) dry and (c) humid (50% RH) conditions. The reaction time is 12 h.

the insoluble MgO core since it needs a parameter of solution density. However, we can directly obtain water contents at different relative humidities. For example, at 90% RH, water contents for HAc reacted MgO particles under dry and humid conditions are 48% and 73%, respectively, while it is only 3% for fresh particles. This demonstrates that the presence of magnesium acetate significantly enhances the water absorption capacity of reacted particles.

Fig. 8 shows the water adsorption isotherms of fresh and HAc reacted $CaCO_3$ particles as well as $Ca(CH_3COO)_2$ particles. For fresh $CaCO_3$ particles (Fig. 8a), the relative humidity corresponding to one monolayer of water adsorbed is $\sim$52% RH while there are approximately 2 layers of adsorbed water at 90% RH and 7 layers at 95% RH. These results are consistent with previous FTIR experiments,[44] thermogravimetric analysis measurements,[47] and Hygroscopic Tandem Differential Mobility Analyzer results.[49] Compared to fresh $CaCO_3$, particles reacted with HAc under dry condition shows a slight increase in water content (Fig. 8b). For example, water content at 90% RH is less than 0.1% for fresh particles and $\sim$2% for acetic acid reacted particles, respectively. Since the reaction between HAc and $CaCO_3$ under dry conditions is limited to the surface as discussed above, few bulk acetate components are formed, which limited the enhancement of the water absorption capacity of reacted particles.

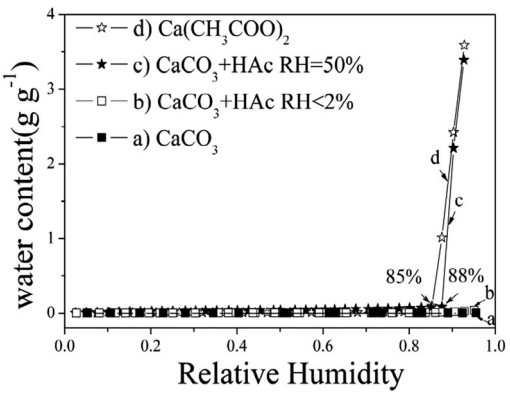

Fig. 8 Adsorption isotherms at 278 K of water on: (a) fresh $CaCO_3$; HAc reacted $CaCO_3$ under (b) dry and (c) humid conditions; and (d) $Ca(CH_3COO)_2$ particles. The reaction time is 12 h.

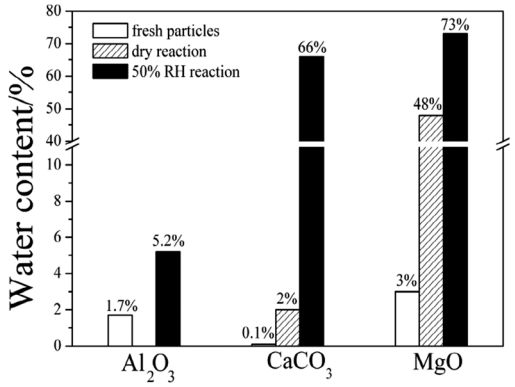

Fig. 9 Comparison of water contents at 90% RH for α-Al_2O_3, $CaCO_3$, and MgO particles with different states: fresh; dry reaction; and 50% RH reaction with HAc for 12 h.

For $CaCO_3$ particles reacted with HAc at 50% RH (Fig. 8c), as well as pure calcium acetate particles (Fig. 8d), a slight enhancement of water absorption was seen for these particles at low humidity. However, the internally mixed $Ca(CH_3COO)_2/CaCO_3$ particles produced in the humid reaction exhibit a clear deliquescence point at ~88% RH, which is very close to 85% RH, the DRH of pure $Ca(CH_3COO)_2$ particles. This implies that the hygroscopic behavior of $Ca(CH_3COO)_2$ in the mixtures is similar to that of pure $Ca(CH_3COO)_2$ particles. The water contents at 90% RH for pure $Ca(CH_3COO)_2$ and internally mixed $Ca(CH_3COO)_2/CaCO_3$ particles were ~70% and ~66%, respectively. The slight discrepancy is due to the presence of insoluble $CaCO_3$ core. In a previous study, Liu *et al.* found that the hygroscopic behavior of $Ca(NO_3)_2/CaCO_3$ particles is identical to that of pure $Ca(NO_3)_2$ particles, suggesting a negligible effect of the slightly soluble $CaCO_3$ inclusion on the hygroscopic behavior of $Ca(NO_3)_2/CaCO_3$ particles.[19] In the present study, the effect of HAc reaction on the hygroscopic property of $CaCO_3$ is similar to that of HNO_3 by producing a $Ca(CH_3COO)_2/CaCO_3$ mixture.

The water contents at 90%RH for α-Al_2O_3, $CaCO_3$, and MgO particles were further compared in different states, as shown in Fig. 9. It can be obviously seen that the effect of the HAc reaction on the hygroscopic behavior of mineral particles depends greatly on the mineralogy of the particles as well as the reaction conditions. This difference is also related to the reaction mechanisms of different particles. These results suggest that heterogeneous reactions of HAc on MgO or $CaCO_3$ under humid conditions are greater than those on α-Al_2O_3 particles.

4. Conclusions and atmospheric implications

Heterogeneous reactions of HAc on α-Al_2O_3, MgO, and $CaCO_3$ under dry or humid conditions as well as the effect on the hygroscopic behavior of these particles has been studied. Acetic acid can react with all these particles. An internally mixed acetate was formed and enhanced the water adsorption/absorption capability of particles. Besides, these mineral particles also exhibited a difference in their reaction mechanism and hygroscopicity change. As for α-Al_2O_3, the reaction was limited to particle surfaces under both dry and humid conditions with the product of surface coordinated acetate species. The water adsorption capacity of α-Al_2O_3 particles increased after the reaction with HAc. However, no deliquescence was observed for HAc reacted α-Al_2O_3 particles. For MgO, $Mg(CH_3COO)_2$ was formed in the reaction with HAc under both dry and humid conditions. The water contents at 90% RH of internally mixed $Mg(CH_3COO)_2/MgO$ particles formed under dry and humid conditions increased to 48% and 73%, respectively. For $CaCO_3$, a little surface acetate was formed under dry conditions, which slightly increased the water content of the mixed particles. When the reaction was under humid conditions, decomposition of bulk $CaCO_3$ occurred. The internally mixed $Ca(CH_3COO)_2/CaCO_3$ particles deliquesced at ~88% RH which is close to 85% RH, the DRH of pure $Ca(CH_3COO)_2$ particles.

Based on the uptake coefficients of formic acid, acetic acid, and propionic acid on α-Al_2O_3 particles, Tong *et al.*[35] determined that the loss of atmospheric monocarboxylic acid due to reactive uptake on mineral dust particles may be competitive with homogeneous loss pathways. In the present study, we found that the reaction extent of acetic acid with MgO and $CaCO_3$ is greater than that with α-Al_2O_3 under atmospheric humidity conditions, which means that the losses of acetic acid on MgO and $CaCO_3$ are larger than those on α-Al_2O_3. Therefore, the loss of acetic acid due to heterogeneous reaction on mineral dust particles may be underestimated by Tong *et al.*

On the other hand, reaction with HAc can also promote the hydrophilic properties of mineral dust. The enhancement of water content in mineral particles can further facilitate heterogeneous and multiphase reactions with other gas pollutants, especially soluble gases (*e.g.* NO_2, HNO_3, SO_2, *etc.*). These results may help the understanding of observed correlations between particulate acetate and nitrate or sulfate.

Acknowledgements

This research was supported by the National Natural Science Foundation of China (No. 21107129, 20937004, 50921064).

Notes and references

1 I. Tegen and I. Fung, *J. Geophys. Res.*, 1994, **99**, 22897–22914.
2 F. Dentener, G. Carmichael, Y. Zhang, J. Lelieveld and P. Crutzen, *J. Geophys. Res.*, 1996, **101**, 22869–22889.
3 IPCC. "IPCC Fourth Assessment Report: Working Group I Report The Physical Science Basis", 2007.
4 D. Cziczo, D. Murphy, P. Hudson and D. Thomson, *J. Geophys. Res.*, 2004, **109**, D04201.
5 R. Duce, C. Unni, B. Ray, J. Prospero and J. Merrill, *Science*, 1980, **209**, 1522.
6 A. R. Ravishankara, *Science*, 1997, **276**, 1058–1065.
7 C. R. Usher, A. E. Michel and V. H. Grassian, *Chem. Rev.*, 2003, **103**, 4883–4940.
8 Y. Zhang and G. Carmichael, *J. Appl. Meteorol.*, 1999, **38**, 353–366.
9 C. Liu, Q. Ma, Y. Liu, J. Ma and H. He, *Phys. Chem. Chem. Phys.*, 2012, **14**, 1668–1676.
10 Q. Ma, Y. Liu and H. He, *J. Phys. Chem. A*, 2008, **112**, 6630–6635.
11 D. Zhang, G. Shi, Y. Iwasaka and M. Hu, *Atmos. Environ.*, 2000, **34**, 2669–2679.
12 A. Laskin, M. Iedema, A. Ichkovich, E. Graber, I. Taraniuk and Y. Rudich, *Faraday Discuss.*, 2005, **130**, 453–468.

13 R. Sullivan, S. Guazzotti, D. Sodeman and K. Prather, *Atmos. Chem. Phys.*, 2007, **7**, 1213–1236.
14 W. J. Li and L. Y. Shao, *Atmos. Chem. Phys.*, 2009, **9**, 1863–1871.
15 W. J. Li and L. Y. Shao, *J. Geophys. Res.*, 2010, **115**, D02301.
16 H. A. Al-Abadleh, B. J. Krueger, J. L. Ross and V. H. Grassian, *Chem. Commun.*, 2003, 2796–2797.
17 B. J. Krueger, V. H. Grassian, M. J. Iedema, J. P. Cowin and A. Laskin, *Anal. Chem.*, 2003, **75**, 5170–5179.
18 B. J. Krueger, V. H. Grassian, A. Laskin and J. P. Cowin, *Geophys. Res. Lett.*, 2003, **30**, 1148.
19 Y. J. Liu, T. Zhu, D. F. Zhao and Z. F. Zhang, *Atmos. Chem. Phys.*, 2008, **8**, 7205–7215.
20 H. A. Al-Abadleh, H. A. Al-Hosney and V. H. Grassian, *J. Mol. Catal. A: Chem.*, 2005, **228**, 47–54.
21 A. Chebbi and P. Carlier, *Atmos. Environ.*, 1996, **30**, 4233–4249.
22 K. Kawamura, L. Ng and I. Kaplan, *Environ. Sci. Technol.*, 1985, **19**, 1082–1086.
23 R. Talbot, K. Beecher, R. Harriss and R. Cofer, *J. Geophys. Res.*, 1988, **93**, 1638–1652.
24 S. Yu, *Atmos. Res.*, 2000, **53**, 185–217.
25 D. Grosjean, *Environ. Sci. Technol.*, 1989, **23**, 1506–1514.
26 S.-H. Lee, D. M. Murphy, D. S. Thomson and A. M. Middlebrook, *J. Geophys. Res.*, 2002, **107**, 4003.
27 L. M. Russell, S. F. Maria and S. C. B. Myneni, *Geophys. Res. Lett.*, 2002, **29**, 1779.
28 S.-H. Lee, D. M. Murphy, D. S. Thomson and A. M. Middlebrook, *J. Geophys. Res.*, 2003, **108**, 8417.
29 C. Sabbioni, N. Ghedini and A. Bonazza, *Atmos. Environ.*, 2003, **37**, 1261–1269.
30 S. Carlos-Cuellar, P. Li, A. P. Christensen, B. J. Krueger, C. Burrichter and V. H. Grassian, *J. Phys. Chem. A*, 2003, **107**, 4250–4261.
31 H. A. Al-Hosney, S. Carlos-Cuellar, J. Baltrusaitis, V. H. Grassian and S. Matter, *Phys. Chem. Chem. Phys.*, 2005, **7**, 3587–3595.
32 C. Hatch, R. Gough and M. Tolbert, *Atmos. Chem. Phys.*, 2007, **7**, 4445–4458.
33 S. Kang and B. Xing, *Langmuir*, 2007, **23**, 7024–7031.
34 A. P. Prince, P. D. Kleiber, V. H. Grassian and M. A. Young, *Phys. Chem. Chem. Phys.*, 2008, **10**, 142–152.
35 S. R. Tong, L. Y. Wu, M. F. Ge, W. G. Wang and Z. F. Pu, *Atmos. Chem. Phys.*, 2010, **10**, 7561–7574.
36 Q. X. Ma, Y. C. Liu and H. He, *J. Phys. Chem. A*, 2010, **114**, 4232–4237.
37 C. Xu and B. Koel, *J. Chem. Phys.*, 1995, **102**, 8158–8166.
38 K. Ito and H. Bernstein, *Can. J. Chem.*, 1956, **34**, 170–178.
39 A. Musumeci, R. Frost and E. Waclawik, *Spectrochim. Acta, Part A*, 2007, **67**, 649–661.
40 Y. C. Liu, Q. X. Ma and H. He, *Atmos. Chem. Phys.*, 2009, **9**, 6273–6286.
41 L. Y. Wang, Y. H. Zhang and L. J. Zhao, *J. Phys. Chem. A*, 2005, **109**, 609–614.
42 H. A. Al-Abadleh and V. H. Grassian, *J. Phys. Chem. B*, 2003, **107**, 10829–10839.
43 H. A. Al-Hosney and V. H. Grassian, *J. Am. Chem. Soc.*, 2004, **126**, 8068–8069.
44 H. A. Al-Hosney, V. H. Grassian and S. Matter, *Phys. Chem. Chem. Phys.*, 2005, **7**, 1266–1276.
45 A. P. Prince, P. Kleiber, V. H. Grassian and M. A. Young, *Phys. Chem. Chem. Phys.*, 2007, **9**, 3432–3439.
46 Y. C. Liu, C. Liu, J. Z. Ma, Q. X. Ma and H. He, *Phys. Chem. Chem. Phys.*, 2010, **12**, 10896–10903.
47 R. J. Gustafsson, A. Orlov, C. L. Badger, P. T. Griffiths, R. A. Cox and R. M. Lambert, *Atmos. Chem. Phys.*, 2005, **5**, 3415–3421.
48 A. L. Goodman, E. T. Bernard and V. H. Grassian, *J. Phys. Chem. A*, 2001, **105**, 6443–6457.
49 E. R. Gibson, P. K. Hudson and V. H. Grassian, *J. Phys. Chem. A*, 2006, **110**, 11785–11799.